

Supporting information for

Nanoelicitors with prolonged retention and sustained release to produce beneficial compounds in wine

Belén Parra-Torrejón^a, Gloria B. Ramírez-Rodríguez,^{a,*} Maria J. Gimenez-Bañon,^b
Juan D. Moreno-Olivares,^b Diego F. Paladines-Quezada,^b Rocío Gil-Muñoz,^b
José M. Delgado-López^{a,*}

^a Departamento de Química Inorgánica, Facultad de Ciencias, Universidad de Granada,
Av. Fuente Nueva, s/n, 18071 Granada, Spain.

^b Instituto Murciano de Investigación y Desarrollo Agroalimentario, Ctra. La Alberca
s/n, 30150, Murcia, Spain.

(*) Authors to whom any correspondence should be addressed: J.M.D.-L.

(jmdl@ugr.es); G.B.R.-R. (gloria@ugr.es)

Table of contents

S1. MeJ quantification by UV-Vis spectroscopy

Fig. S1.

Fig. S2.

Fig. S3.

Fig. S4.

Fig. S5.

Fig. S6.

Fig. S7.

Fig. S8.

Table S1.

Table S2.

S1. MeJ quantification by UV-Vis spectroscopy

MeJ ketone group strongly absorbs in the UV region near $\lambda = 291$ nm and its ester group absorbs at $\lambda = 214$ nm (Figure S1a).¹ We selected the former absorption band for the calibration curves. Taking into account the low solubility of MeJ, we carried out two calibration curves: (1) 100-800 ppm in ultrapure water (Figure S1b, green dots) and (2) 100-2000 ppm ultrapure water:ethanol (50:50, Figure S1b, blue dots). The fitting parameters for each curves are:

$$Abs = 1.73 \cdot 10^{-4} [MeJ] + 0.0078 \quad R^2 = 0.99 \quad (1)$$

$$Abs = 2.07 \cdot 10^{-4} [MeJ] - 0.0028 \quad R^2 = 0.99 \quad (2)$$

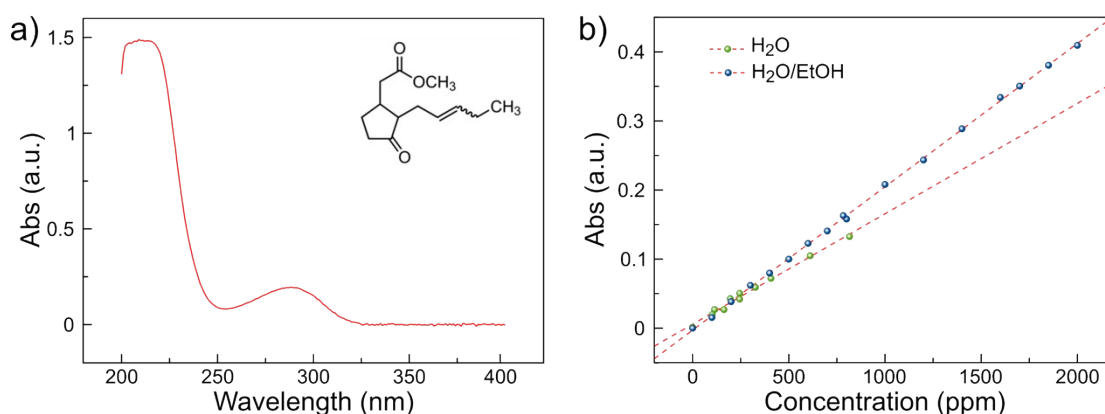


Fig. S1 UV-Vis spectrum (a) and calibration curve (b) of methyl jasmonate in H₂O (green dots) and H₂O/EtOH (1:1, blue dots). Dashed lines represent the best fits of the experimental data according to equation 1 for H₂O and equation 2 for H₂O/EtOH.

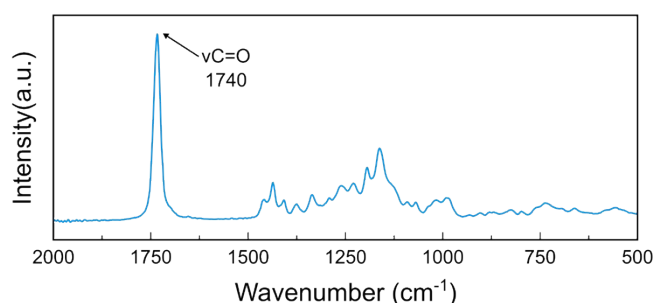


Fig. S2 FTIR spectrum of MeJ showing the most intense absorption band at 1740 cm⁻¹ corresponding to carbonyl (ketone) groups.²

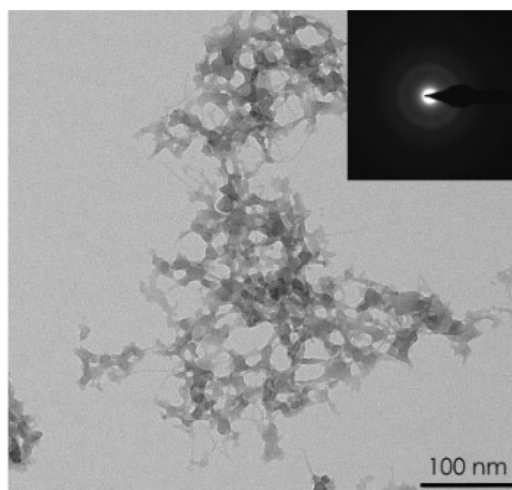


Fig. S3 TEM micrograph of nano-MeJ. The nanoparticles shows the same morphology than control ACP nanoparticles.³ The amorphous nature of the particles is confirmed by the lack of diffraction spots in the selected-area electron diffraction (SAED) pattern (inset).

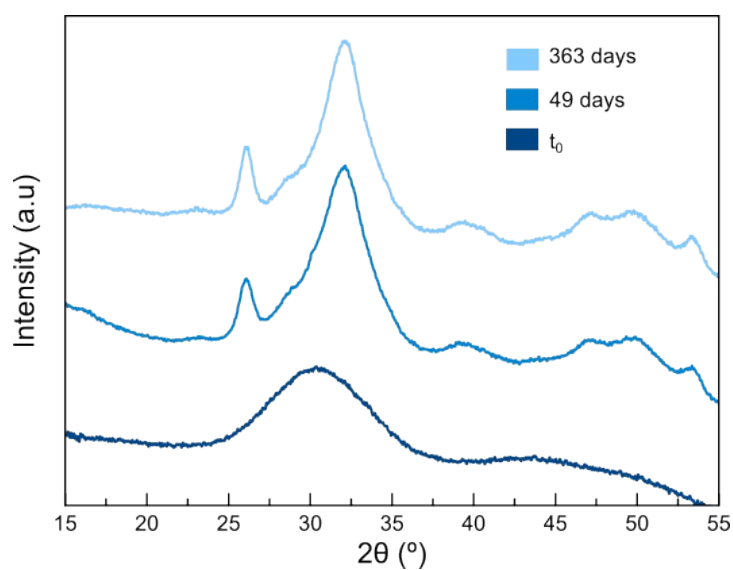


Fig. S4 XRD patterns of nano-MeJ sample freeze-dried at time 0, 49 and after 363 days. XRD patterns after 49 and 363 days of storage show two broad Bragg peaks at around 26° and 32° (2θ) ascribed to hydroxyapatite (HA, ASTM card file No 09-432).

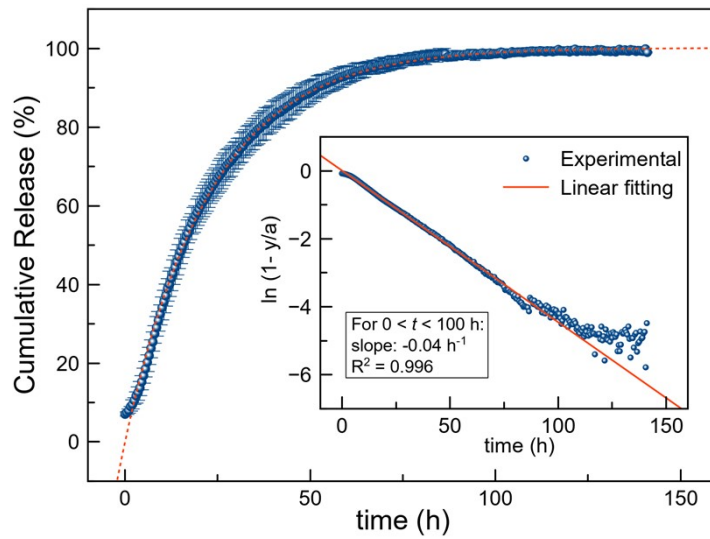


Fig. S5 MeJ release profile from nano-MeJ in ultrapure water. Dashed line represents the best fits of the experimental data to the first order equation: $y(t) = a*(1-e^{-kt})$, being the rate constant, $k = 0.05 \text{ h}^{-1}$. The inset shows the linearized experimental data (symbols) and the first order equation (line).

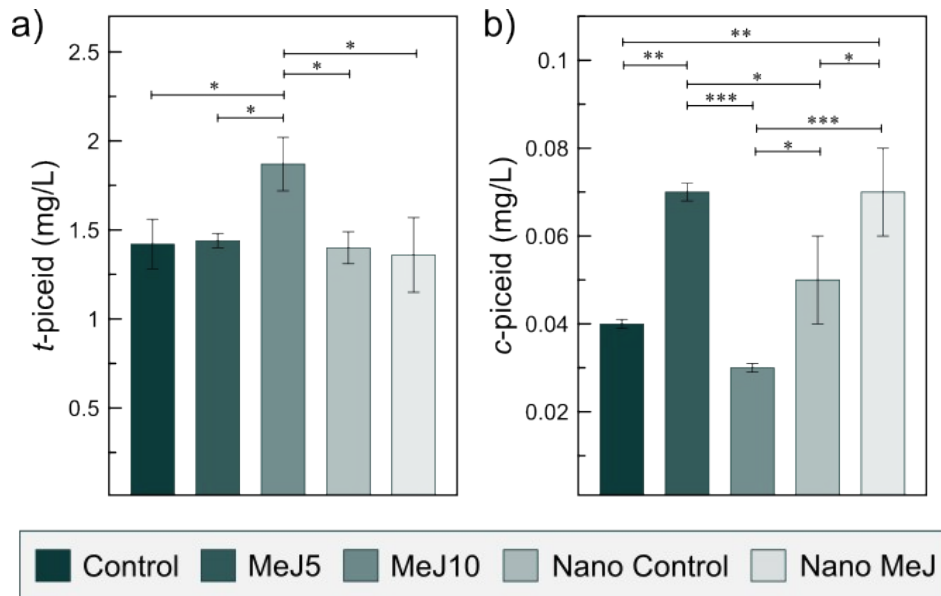


Fig. S6 (a) *t*-piceid and (b) *c*-piceid concentration (mg L^{-1}) in wines from grapes treated with MeJ (5 mM, MeJ5, and 10 mM, MeJ10) and nano-MeJ with a total concentration of 1 mM. Results of grapes treated with ACP nanoparticles (nano-Control) and non-treated grapes (control) are also shown. Data are expressed as mean with their corresponding standard deviation as error bars. Statistically significant differences between measurements are marked with * (P-value < 0.05), ** (P-value < 0.01) or *** (P-value < 0.001).

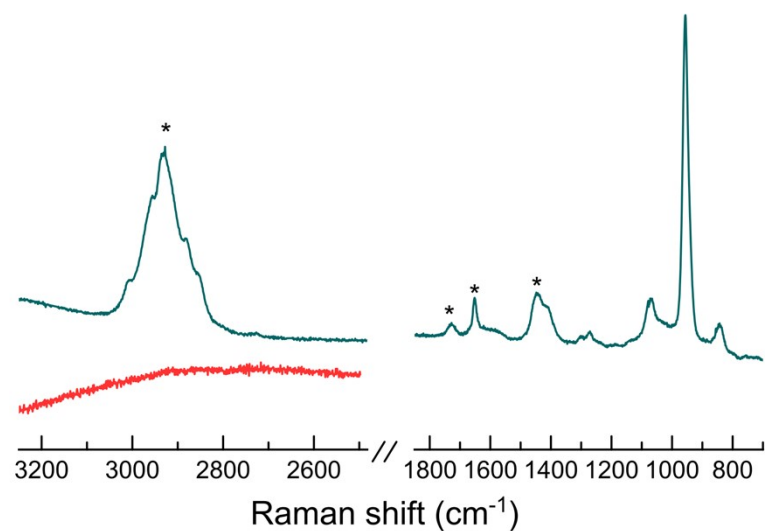


Fig. S7 Raman spectroscopy of 10 mM MeJ (red spectrum) and NanoMeJ (blue spectrum) after 24 hours at 50°C. Asterisks indicate the presence of MeJ.

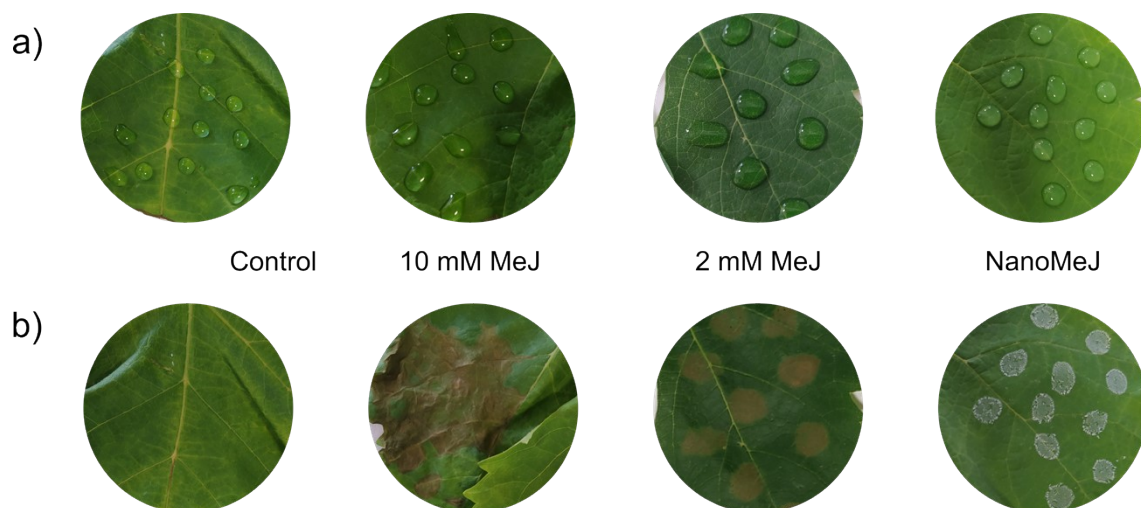


Fig. S8. Images of vineyards leaves treated with water (Control), MeJ solution (10 and 2 mM) and NanoMeJ (2 mM) at time zero (a) and after 24 hours (b).

Table S1. Chemical composition and ζ -potential of nano-MeJ and ACP nanoparticles (nano-Control). Data are expressed as mean \pm standard deviation.

| | Ca ^a (wt.%) | P ^a (wt.%) | K ^a (wt.%) | Ca/P ^a | ζ ^b (mV) | MeJ ^c (wt.%) |
|--------------|---------------------------|--------------------------|--------------------------|-------------------|------------------------------|----------------------------|
| Nano-MeJ | 18.02 \pm 4.3 | 8.79 \pm 1.3 | 0.27 \pm 0.01 | 1.57 \pm 0.13 | -15.7 \pm 0.6 | 6.15 \pm 1.71 |
| Nano-Control | 14.7 \pm 0.14 | 8.06 \pm 0.1 | 0.46 \pm 0.01 | 1.41 \pm 0.03 | -10.3 \pm 0.7 | - |

^aAnalysed by ICP-OES. ^bAnalysed by Litesizer 500. ^cEstimated by UV-Vis spectroscopy

Table S2. Enological parameters of the must from grapes under each treatment. Statistically significant differences between measurements are marked with ** (P-value < 0.01) whereas ns means no statistical differences.

| | Control | Nano-Control | MeJ | Nano-MeJ | P |
|------------------------|----------------|----------------|----------------|----------------|----|
| °Baumé | 12.9 \pm 0.4 | 13.1 \pm 0.2 | 12.8 \pm 0.2 | 12.9 \pm 0.4 | ns |
| Total Acidity (g/L) | 2.8 \pm 0.2b | 2.5 \pm 0.1c | 3.2 \pm 0.2a | 2.9 \pm 0.1b | ** |
| pH | 3.9 \pm 0.1 | 3.9 \pm 0.1 | 3.8 \pm 0.1 | 3.9 \pm 0.1 | ns |

References

- 1 J. Islam, S. Phukan and P. Chattopadhyay, Development of a validated RP-HPLC/DAD method for the quantitative determination of methyl jasmonate in an insect repellent semi-solid formulation, *Heliyon*, 2019, **5**, e01775.
- 2 T. Sato, T. Kawara, K. Sakata and T. Fujisawa, Jasmonoid Synthesis from sci-4-Heptenoic Acid, *Bull. Chem. Soc. Jpn.*, 1981, **54**, 505–508.
- 3 G. B. Ramírez-Rodríguez, G. Dal Sasso, F. J. Carmona, C. Miguel-Rojas, A. Pérez-de-Luque, N. Masciocchi, A. Guagliardi and J. M. Delgado-López, Engineering Biomimetic Calcium Phosphate Nanoparticles: A Green Synthesis of Slow-Release Multinutrient (NPK) Nanofertilizers, *ACS Appl. Bio Mater.*, 2020, **3**, 1344–1353.